Redox Polyelectrolytes with pH-Sensitive Electroactive Functionality in Aqueous Media

Kai-Jher Tan, Satoshi Morikawa, Nil Ozbek, Magdalena Lenz, Carsten-René Arlt, André Tschöpe, Matthias Franzreb, and T. Alan Hatton*

ABSTRACT: A framework of ferrocene-containing polymers bearing adjustable pH- and redox-active properties in aqueous electrolyte environments was developed. The electroactive metallopolymers were designed to possess enhanced hydrophilicity compared to the vinylferrocene (VFc) homopolymer, poly(vinylferrocene) (PVFc), by virtue of the comonomer incorporated into the macromolecule, and could also be prepared as conductive nanoporous carbon nanotube (CNT) composites that offered a variety of different redox potentials spanning a ca. 300 mV range. The presence of charged non-redox-active moieties such as methacrylate (MA) in the polymeric structure endowed it with acid dissociation properties that interacted synergistically with the redox activity of the ferrocene moieties to impart pH-dependent electrochemical behavior to the overall polymer, which was subsequently studied and compared to several Nernstian relationships in both homogeneous and heterogeneous configurations. This zwitterionic characteristic was leveraged for the enhanced electrochemical separation of several transition metal oxyanions using a P($VFc_{0.63}$-*co*-$MA_{0.37}$)-CNT polyelectrolyte electrode, which yielded an almost twofold preference for chromium as hydrogen chromate versus its chromate form, and also exemplified the electrochemically mediated and innately reversible nature of the separation process through the capture and release of vanadium oxyanions. These investigations into pH-sensitive redox-active materials provide insight for future developments in stimuli-responsive molecular recognition, with extendibility to areas such as electrochemical sensing and selective separation for water purification.

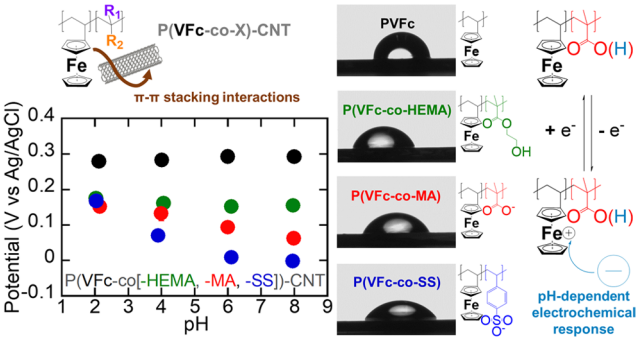

INTRODUCTION

Redox-active species find great application in a plethora of areas, with the most notable being energy storage,[1] sensing,[2] catalysis,[3] and more recently, the burgeoning field of electrochemically mediated separation techniques.[4,5] The unique nature of these compounds allows their oxidation states to be altered chemically or through the more utile approach of an electrochemical stimulus. Molecular recognition is a key requirement for many redox-based processes.[6] Electrochemical sensors can be designed to identify species in both the liquid and gaseous states,[7] and have been employed in aqueous environments for pH determination,[8] as well as in organic media.[9] As solution matrices are often composed of many constituents, a clear degree of selectivity for the analyte of interest is required. This can be manifested in the form of highly specific redox reactions to facilitate characterizable electrochemically mediated phenomena such as species transformation,[10] intercalation,[11] or binding.[12] From a design perspective, materials that possess the innate ability to activate via a simple electrochemical stimulus for reversible binding with certain molecules are particularly desirable for analyte detection due to their inherent electronic tunability, which enables the precise control of their redox properties for targeted interactions.

Redox-active macromolecules have previously been developed and investigated as potential materials for electrochemically mediated analyte targeting.[4,13] Specificity can be imparted through molecular imprinting techniques[14] but can also be an innate property. For example, coordination polymers such as transition metal hexacyanoferrates and metal−organic frameworks have been shown to be able to electrochemically detect metal ions,[15] conducting polymers have been utilized for gas sensing,[16] and polymeric quinones have exhibited pH- and carbon dioxide-dependent electroactive responses.[17] Metallopolymers have also been applied to electrochemical gas and

cation recognition,[18,19] with polyferrocenes in particular being leveraged as molecular receptors[20] because of their redox-mediated affinities for the determination of glucose,[21] as well as the separation of numerous organic and inorganic anions.[22−27]

Ferrocene is the archetypal redox-active molecule and is an organometallic compound that exists as a facile and reversible redox couple with its oxidized ferrocenium counterpart.[28] This process involves the generation of a complex between the ferrocenium cation and an anion, with the nature of the anion influencing the ease with which ferrocene oxidizes to form an ion pair, and hence, its electrochemical response.[29,30] The redox-active behavior of ferrocene species has been studied through their dissolution in homogeneous solution,[31] as well as heterogeneously, via surfaces possessing covalently bound moieties,[29,30] or in the form of a redox polymer.[32,33] The discovery of poly(vinylferrocene) (PVFc), one of the simplest ferrocene homopolymers,[34] has been subsequently followed by the development of a multitude of ferrocene-containing macromolecules.

Metallopolymers possessing ferrocene derivatives as their source of redox activity have been formulated through a variety of methods, including techniques such as postpolymerization addition of pendant ferrocene units and copolymerization of ferrocenyl monomers with other monomers.[35] In the case of the latter, ferrocene in its vinylferrocene form has been used in combination with other vinyl species to generate ferrocene copolymers with an extended alkane chain backbone.[33,36,37] Although previous studies of such copolymers have assessed the retained performance of the redox-active properties of the ferrocene groups, their applicability to electrochemical systems as a whole can be expanded and enhanced by leveraging their multimonomer design framework to introduce additional functionality.

In this work, a series of ferrocene copolymers possessing adjustable overall hydrophilicity based on the chemical structure of non-redox-active components (i.e., 2-hydroxyethyl methacrylate, methacrylate, or 4-styrene sulfonate) incorporated within the polymers was developed. The use of acid functional groups together with the ferrocene moieties engendered pH-sensitive electrochemical behavior that was investigated through dissolution of the polyelectrolyte as well as its noncovalent attachment onto a carbon nanotube network at an electrode interface. Furthermore, this property was used to augment the electrochemical separation ability of the overall polymer by facilitating preferential electrosorption of heavy metal chromium and vanadium oxyanions under different solution conditions. Although there are many well-known intrinsically pH-dependent redox-active species that display proton-coupled electron transfer (PCET) reactions,[38,39] electroactive materials can also be made to possess indirect pH-dependent electrochemistry by design,[40−45] with examples including redox-active polyelectrolytes and self-assembled monolayers,[46−51] and dual pH- and redox-responsive polymers for drug delivery that typically employ the redox-mediated cleavage of disulfide linkages.[52] The pH-sensitive zwitterionic ferrocene polymers in this study utilize traditionally pH-independent redox-active moieties, and this alternative approach of leveraging the synergistic interplay between acid dissociation and redox properties offers additional dimensionality in the design of future techniques and materials for electrochemical molecular recognition and water remediation.

EXPERIMENTAL SECTION

The ferrocene polymers described in this study were prepared through free-radical polymerization of vinylferrocene (VFc) by itself, or with a comonomer, i.e., 2-hydroxyethyl methacrylate (HEMA), methacrylate (MA), or 4-styrene sulfonate (SS). The synthesis procedures were developed from previously reported methodologies for the free-radical polymerization of vinylferrocene-containing polymers.[33,36,37] Briefly, PVFc, P(VFc_{1-m}-*co*-$HEMA_m$), and P(VFc_{1-m}-*co*-MA_m) were generally synthesized in anhydrous 1,4-dioxane at 70 °C with a total monomer concentration of ca. 10 M and ca. 10 mol % (with respect to the total monomer amount) of 2,2′-azobis(2-methylpropionitrile) (AIBN) as the radical initiator, unless otherwise specified in the Supporting Information. P(VFc-*co*-SS) was synthesized under the same conditions but with a total monomer concentration of ca. 2 M and ca. 5 mol % of AIBN.

Polymer electrodes were made using two different approaches. Conductive ferrocene polymer composites were generated by dispersing the polymers together with multiwalled carbon nanotubes (CNTs) using a method adapted from previously reported noncovalent functionalization techniques.[19,22,25,53] Briefly, the ferrocene polymer and CNTs were added to *N*,*N*-dimethylformamide (DMF) and sonicated for at least 3 h in a ratio of 4 mg of VFc units and 4 mg of CNTs per 1 mL of DMF. P(VFc_{1-m}-*co*-X_m)-CNT electrodes were then made by drop-casting 50 μL of the resulting dispersion onto conductive Teflon-coated carbon fibers and drying the solvent to generate a film. For the pH-based electrochemical separations, an additional 50 μL of the dispersion was drop-cast on the other side of the carbon fibers and subsequently dried to yield a two-sided 100 μL dispersion electrode. The reversible vanadium capture and release experiment and all other electrochemical characterizations utilized single-sided 50 μL dispersion electrodes. For the P(VFc_{1-m}-*co*-$HEMA_m$) redox potential experiment, P(VFc_{1-m}-*co*-$HEMA_m$) electrodes without carbon nanotubes were prepared by dissolving the polymers in DMF in a ratio of 4 mg of VFc units per 1 mL of DMF, drop-casting 5 μL of the resulting solution onto conductive carbon fibers, and drying the solvent to generate a film.

Electrochemical characterization was carried out using a three-electrode setup with a platinum wire counter electrode and an Ag/Ag^+ reference electrode under quiescent conditions in a ca. 20 mL cylindrical glass vial with either 4 or 5 mL of solution. Electrochemical separations were performed using a three-electrode setup with a platinum wire counter electrode and an Ag/AgCl reference electrode under stirred conditions in a rectangular base cuvette cell (ca. 2.5 × 3.8 × 1 cm) with 2 mL of solution, with the exception of the reversible vanadium capture and release experiment, for which a square base cuvette cell (ca. 1.25 × 1.25 × 4.5 cm) and 1.5 mL of solution were used. Solution concentrations before and after the operation of electrochemical processes were assessed using inductively coupled plasma-optical emission spectroscopy (ICP-OES).

Buffered aqueous solutions for pH experiments were prepared using a modified Britton−Robinson buffer system. In an effort to mitigate the effects of changes in the buffer ionic strength from pH adjustment, additional $NaClO_4$ supporting electrolyte was included in each pH solution at a concentration of 0.5 M to saturate their ionic strengths.

Further details on preparation methods and characterization can be found in the Supporting Information.

RESULTS AND DISCUSSION

Ferrocene Copolymers (P(VFc_{1-m}-*co*-X_m)). Random polymers of vinylferrocene (VFc) containing 2-hydroxyethyl methacrylate (HEMA), methacrylate (MA), or 4-styrene sulfonate (SS) moieties were prepared (Figure 1a) using different methods, as well as with varying comonomer compositions. The straightforward approach of free-radical copolymerization was selected to facilely incorporate non-redox-active moieties alongside vinylferrocene for the convenient assessment of their effects on the properties of the

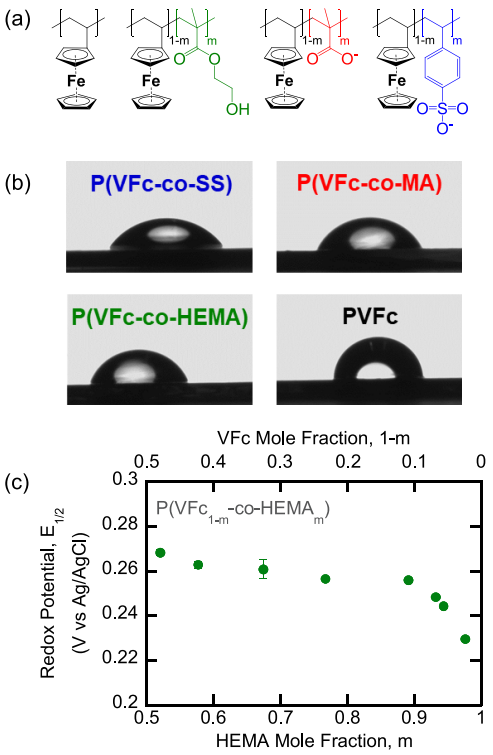

Figure 1. (a) Chemical structures of the hydrophilic ferrocene copolymers, P(VFc$_{1-m}$-*co*-X_m). From left to right: PVFc, P(VFc-*co*-HEMA), P(VFc-*co*-MA), and P(VFc-*co*-SS). (b) Images for contact angle measurements of P(VFc-*co*-*X*) with deionized water. (c) Redox potentials of P(VFc$_{1-m}$-*co*-HEMA$_m$) as a function of HEMA monomer mole fraction, *m*, obtained from cyclic voltammetry after five cycles at 0.01 V/s in 0.1 M $NaClO_4$ aqueous solution.

overall polymer. The resulting ferrocene copolymers are described with the P(VFc$_{1-m}$-*co*-X_m) naming convention, where *m* is the mole fraction of comonomer *X* in the polymer. Unless explicitly labeled, the generic P(VFc-*co*-*X*) designation without specified mole fractions refers to copolymers containing ca. 30 mol % VFc or *m* = ca. 0.70 (i.e. P(VFc$_{0.33}$-*co*-HEMA$_{0.67}$) for P(VFc-*co*-HEMA), P(VFc$_{0.36}$-*co*-MA$_{0.64}$) for P(VFc-*co*-MA), and P(VFc$_{0.31}$-*co*-SS$_{0.69}$) for P(VFc-*co*-SS)).

Poly(vinylferrocene-*co*-4-styrene sulfonate) (P(VFc-*co*-SS)) was synthesized via the direct copolymerization of VFc and tetrabutylammonium 4-styrene sulfonate (TBASS), where TBASS was obtained by reacting sodium 4-styrene sulfonate (NaSS) with tetrabutylammonium hydroxide (TBAOH) (Figure S1, SI).[54] The cation exchange step was performed to render the 4-styrene sulfonate monomer soluble in the 1,4-dioxane polymerization solvent, and the completion of the reaction was confirmed by comparing the TBASS and NaSS signals (Figure S2a, SI), as well as the ratios of the tetrabutylammonium and styrene sulfonate signals in TBASS from ^{1}H nuclear magnetic resonance (NMR) spectroscopy (Figure S2b, SI).

Poly(vinylferrocene-*co*-methacrylate) (P(VFc$_{1-m}$-*co*-MA$_m$)) species were synthesized using a postpolymerization deprotection approach. Specifically, VFc was first copolymerized with (trimethylsilyl)methacrylate (TMSMA) to obtain poly(vinylferrocene-*co*-(trimethylsilyl)methacrylate) (P(VFc$_{1-m}$-*co*-TMSMA$_m$)), which was then hydrolyzed with alcohol to remove the trimethylsilyl groups,[55] leaving behind methacrylic acid (MAA) moieties and yielding P(VFc$_{1-m}$-*co*-MA$_m$) (Figure S3, SI). The completion of the hydrolysis reaction was confirmed through ^{1}H NMR spectroscopy (Figure S4, SI). However, as TMSMA can react even with moisture in ambient air,[56] it is likely that the starting TMSMA monomer may have already undergone hydrolysis to some extent. Fortunately, this did not affect the ultimate goal of the polymerization, which was to create a VFc copolymer end-product containing MAA units in a ratio commensurate with the monomer feed amounts (Table S1, SI). Copolymerization of VFc with TMSMA was attempted because previous work reported that free-radical polymerization between VFc and MAA resulted in lower yields when higher VFc feed compositions were used, citing the terminating effect of VFc as a radical scavenger.[57]

Poly(vinylferrocene-*co*-2-hydroxyethyl methacrylate) (P(VFc$_{1-m}$-*co*-HEMA$_m$)) species were synthesized via the direct copolymerization of VFc with HEMA,[33] as adapted from previously reported techniques.[36,37]

The polymers were characterized via ^{1}H NMR spectroscopy (Figure S5, SI), ultraviolet−visible (UV−vis) spectroscopy (Figure S6, SI), and infrared (IR) spectroscopy (Figure S7, SI). UV−vis spectroscopy was used to determine the polymer compositions for all the ferrocene copolymers except for P(VFc-*co*-SS), whose VFc amount was determined using ^{1}H NMR spectroscopy as a result of the inability to observe the UV−vis signal of the VFc moiety. The quantification results revealed the presence of VFc moieties and confirmed their amounts to be similar to their corresponding feed quantities (Table S1, SI).

Hydrophilicity of P(VFc$_{1-m}$-*co*-X_m). The hydrophilicities of the synthesized P(VFc$_{1-m}$-*co*-X_m) polymers were assessed via imaging and electrochemical techniques.

The influence of the comonomer was investigated via contact angle measurements. The contact angle of deionized water with P(VFc-*co*-*X*)-treated surfaces yielded a hydrophilicity trend in the order of P(VFc-*co*-SS) > P(VFc-*co*-MA) > P(VFc-*co*-HEMA) > PVFc, where PVFc was the least hydrophilic interface (Figure 1b). The effect of the comonomers on the surface hydrophilicity was apparent, with the P(VFc-*co*-MA) material producing a contact angle of 64.4 ± 0.7°, notably smaller than that of PVFc at 90.9 ± 1.5°.

The effect of comonomer composition was also studied by varying the HEMA-to-VFc ratio at high HEMA mole fractions in the P(VFc$_{1-m}$-*co*-HEMA$_m$) copolymer system (Table S2, SI). Specifically, P(VFc$_{1-m}$-*co*-HEMA$_m$) polymers of different compositions were deposited onto carbon fiber substrates and subjected to heterogeneous cyclic voltammetry to determine the redox potential of each ferrocene polymer in aqueous media from the resulting cyclic voltammograms (CVs). It was observed that although the VFc moiety redox half potential, $E_{1/2}$, stayed roughly constant from ca. *m* = 0.5 to 0.9, it decreased markedly as the mole fraction of HEMA in the polymer approached unity past ca. *m* = 0.9 (Figure 1c). This phenomenon suggests that a higher overall hydrophilicity of the copolymer as imparted by the amount of HEMA groups may allow for greater ease in the oxidation of their ferrocene moiety counterparts.

Electrochemical Behavior of P(VFc-*co*-*X*)-CNT. The redox-active properties of the ferrocene copolymers were analyzed to investigate the influence of the nonredox monomers on the electrochemical behavior of the polymers. The ferrocene copolymers were first combined with multiwalled carbon nanotubes (CNTs) to create conductive P(VFc-*co*-*X*)-CNT electrodes, which conveniently served the twofold

purpose of securing the polymeric species on a heterogeneous surface (via noncovalent pi−pi stacking interactions between VFc cyclopentadienyl rings and the sp^2-hybridized CNT surfaces) and enhancing the electrochemical activation of the VFc moieties.[53,58] PVFc has been found to stabilize both multiwalled and single-walled CNTs in chloroform,[58] and composite films prepared from such dispersions have also been investigated to determine the effect of the PVFc/CNT composition ratio on the specific pseudocapacitance of the resulting electrode.[23,53] Previous studies have employed multiwalled and single-walled CNTs as conduits for functionalized redox-active moieties to perform electrocatalysis, sensing, and energy storage.[59] Scanning electron microscopy (SEM) images of the P(VFc-*co*-MA)-CNT composite revealed a nanostructured morphology with uniform polymer coating of the CNTs (Figure 2a and Figure S8, SI). The P(VFc-*co*-*X*)-CNT materials were also characterized using X-ray photoelectron spectroscopy (XPS), which established the successful incorporation of the polymers within the electrode via the observation of Fe $2p_{1/2}$ and $2p_{3/2}$ signals of the VFc moieties between ca. 705 and 730 eV and the S 2p signal of the P(VFc-*co*-SS) sulfonate groups at ca. 168 eV (Figures S9 and S10, SI).

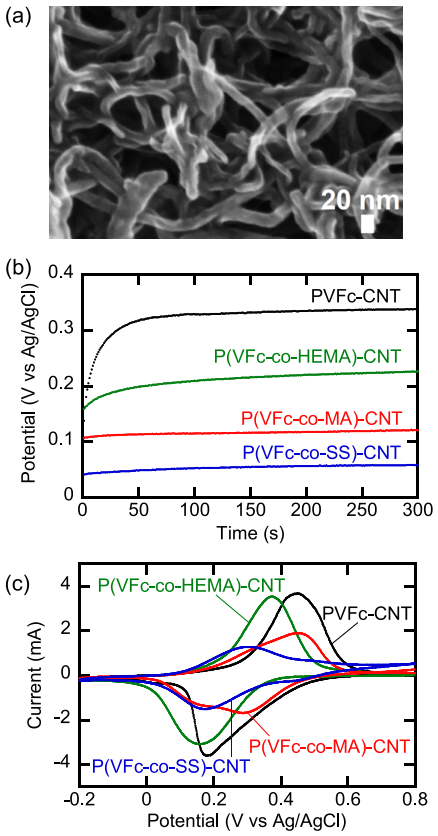

Figure 2. (a) SEM image of P(VFc-*co*-MA)-CNT. (b) Chronopotentiometry experiments with P(VFc-*co*-*X*)-CNT at 2 μA (ca. 0.02 A/m^2) in 0.1 M $NaClO_4$ aqueous solution. (c) Representative CVs of P(VFc-*co*-*X*)-CNT after two cycles at 0.01 V/s in 0.1 M $HClO_4$ aqueous solution.

The effect of the specific comonomer present in the ferrocene polymers was examined through electrochemical testing of the fabricated P(VFc-*co*-*X*)-CNT electrodes. Low-current chronopotentiometry experiments in neutral aqueous media resulted in remarkably distinct electrode potentials spanning an overall range of 280 mV (Figure 2b). Like the heterogeneous electrochemical tests with the P(VFc_{1-m}-*co*-$HEMA_m$) electrodes, there was also an observed correlation between redox potential and the hydrophilicity of the polymer. As the mole fractions of the nonredox monomers in each of the tested polymers were approximately the same, the differences in hydrophilicity were expected to have arisen from the properties of the monomers themselves. To study this further, the redox activities of the P(VFc-*co*-*X*) polymers were studied in different solutions. First, the previous low-current chronopotentiometry experiments were repeated in acidic media at the same ionic strength (Figure S11, SI). It was observed that the electrode potentials were noticeably less distinct, with the potential range halved to ca. 140 mV. Furthermore, the sequential ordering of P(VFc-*co*-*X*)-CNT redox potentials changed as a result of the PVFc-CNT and P(VFc-*co*-HEMA)-CNT potentials staying constant, whereas those of the P(VFc-*co*-MA)-CNT and P(VFc-*co*-SS)-CNT composites increased by differing amounts of 73 and 222 mV, respectively. Previous studies have illustrated that charged polyelectrolyte layers exhibit Donnan potential differences between the electrode interface and the solution,[41,43−45,47,60,61] a concept that would also be in line with the noted increase and absence of an increase in the potentials of P(VFc-*co*-MA)-CNT/P(VFc-*co*-SS)-CNT and PVFc-CNT/P(VFc-*co*-HEMA)-CNT, respectively, when switched from neutral to acidic solution. Heterogeneous CVs of the P(VFc-*co*-*X*)-CNT materials in the same acidic conditions showed clear redox peaks corresponding to the ferrocene moieties in each polymer, with comparable reduction potentials and pseudocapacitances (Figure 2c and Figure S12, SI). Second, homogeneous CVs of the P(VFc-*co*-*X*) polymers were carried out in an organic solvent acting as a polar aprotic proxy for water, namely, *N*,*N*-dimethylformamide (Figure S13, SI). Similar to the experiments in acidic media, the dissolved polymers had a smaller variation in redox potentials than the experiments in neutral media. As such, the observed dissimilarity in the response of the P(VFc-*co*-*X*) polymers to varying solution environments implies that the changes in their electrochemical behavior may correspond to the acid dissociation properties of the nonredox monomers in aqueous media.

Electrochemical pH Response. The effect of pH on the corresponding P(VFc-*co*-*X*) electrochemical response was probed through homogeneous and heterogeneous characterization experiments.

Acidities of Nonredox Comonomers and P(VFc-co-X). The propensity of a chemical species to split into its conjugate base anion and a proton is described by its acid dissociation constant, K_a. For a monoprotic acid, this equilibrium reaction is (eq 1):[62]

$$HA \leftrightarrow A^- + H^+ \tag{1}$$

where HA is the acid, A^- is the anionic conjugate base of the acid, and H^+ is the hydrogen cation. The K_a of eq 1 can subsequently be rewritten in terms of pK_a, which is negatively correlated with the acidic strength of the chemical species (eq 2):[62]

$$pK_a = pH + \log_{10}\frac{[HA]}{[A^-]} \tag{2}$$

It follows that the differences in pK_a among the individual comonomers suggest that their hydrophilicities are governed

by the amounts of hydrophilic anionic groups they form, or in other words, their tendencies to become charged. These pK_a values were calculated using ChemAxon's Chemicalize platform and obtained as −2.13 for 4-stryene sulfonic acid (SSA), 4.86 for methacrylic acid (MAA), and 15.10 for 2-hydroxyethyl methacrylate (HEMA). The trend in acidity varies as SSA > MAA > HEMA, where the least acidic HEMA is unlikely to ionize within a standard aqueous pH range of 0 to 14. As such, this suggests that P(VFc-*co*-HEMA) should not exhibit pH-dependent electrochemical characteristics, whereas the P(VFc-*co*-SS) and P(VFc-*co*-MA) polymers would.

Homogeneous Redox Activity. The redox behavior of acidic ferrocene polymers in solution were assessed via homogeneous voltammetry. Methacrylate-containing ferrocene copolymers at two different compositions, P($VFc_{0.02}$-*co*-$MA_{0.98}$) and P($VFc_{0.05}$-*co*-$MA_{0.95}$), were subjected to cyclic voltammetry in an aqueous solution with ca. 10 vol % methanol added to allow for their complete dissolution at a concentration equal to ca. 1 mM VFc units. Interestingly, it was seen that the Faradaic response of the VFc moieties in the copolymer varied with changes in the apparent pH of the solution. Specifically, the redox-active signal was clearly visible at acidic conditions but became increasingly suppressed at higher apparent pH values, especially in the case of the reduction peak (Figure 3a). This trend, as well as the formation of two reduction peaks at more basic conditions, matched the results from previous studies of ferrocene-labeled acrylic acid and pyridine polymers in homogeneous solution, respectively, with the latter observation being attributed to energy differences required to oxidize ferrocene in the presence of the charged pyridinium.[48,49] To study this phenomenon more carefully, the obtained cyclic voltammograms were first integrated and converted to pseudocapacitance values, and then tracked across an apparent pH range of ca. 2 to 11 (Figure 3b). The magnitudes of both polymer pseudocapacitances decreased with increasing apparent pH and eventually reached a plateau that began at a value approximately equal to the pK_a of methacrylic acid (pK_a = 4.86). The slight discrepancy between the start of the plateau and the pK_a of methacrylic acid was anticipated because of the variation between pK_a values of the acid groups in poly(methacrylic acid) and their individual monomers arising from different electrostatic environments,[63] as well as the presence of methanol in the aqueous solution,[64] with the latter expected to promote less acid dissociation than a purely aqueous solvent.[65] This suggests that a possible mechanism for the observed behavior is that the MAA moieties in the polymers convert to their conjugate base forms to larger extents in more basic solution environments, and subsequently surround and effectively deactivate the ferrocenium groups. As the ferrocene polymer is dissolved in solution, it may be able to freely change its configuration to allow its deprotonated anionic MAA groups to come in proximity and interact with its cationic ferrocenium groups, which would prevent the latter from forming ion pairs with the electrolyte anions and result in a hindered electrochemical response.

To further investigate this hypothesis, two different Nernstian models can be examined for describing the pH-sensitive redox-active properties of the ferrocene polyelectrolyte. In the first framework, both the acid dissociation of the comonomer and the interaction between ferrocenium and anionic species are considered. Specifically, it can be assumed that the one-electron oxidized ferrocenium cationic species in

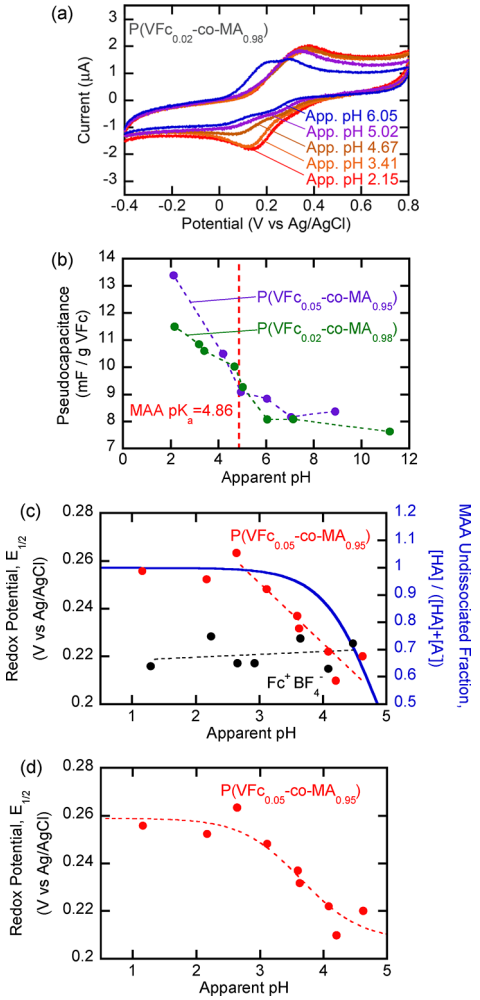

Figure 3. (a) Homogeneous CVs of P($VFc_{0.02}$-*co*-$MA_{0.98}$) under N_2 after 20 cycles at 0.1 V/s in 4 mL of individually prepared 1:9 MeOH/H_2O mixtures (by volume) with differing apparent pH values. (b) Pseudocapacitances of P($VFc_{0.02}$-*co*-$MA_{0.98}$) and P($VFc_{0.05}$-*co*-$MA_{0.95}$) obtained under N_2 after 20 cycles at 0.1 V/s in 4 mL of individually prepared 1:9 MeOH/H_2O mixtures (by volume) with differing apparent pH values. Redox potentials of (c) P($VFc_{0.05}$-*co*-$MA_{0.95}$) and $Fc^+BF_4^-$, and (d) P($VFc_{0.05}$-*co*-$MA_{0.95}$), obtained under N_2 after 10 cycles at 0.2 V/s in 4 mL of individually prepared 1:9 MeOH/H_2O mixtures (by volume) and H_2O for P($VFc_{0.05}$-*co*-$MA_{0.95}$) and $Fc^+BF_4^-$, respectively, with differing apparent pH values. Dotted lines are included to guide the eye of the viewer, with those in (c) representing the lines of best fit for the data points in their corresponding regions, and the one in (d) representing the nonlinear fit of the data points to eq 7 in the main text. For (a) and (b), each solution contained ca. 0.1 M $NaClO_4$, whereas for (c) and (d), each solution contained ca. 0.1 M $HClO_4$. Solutions were pH adjusted if necessary using HCl or NaOH solution.

the dissolved polymer can form ion pairs with two possible anionic species, one being the MAA comonomers present in the polymer structure, and the other being the supporting electrolyte anion present in the solution to increase conductivity for the electrochemical characterization. A generic equilibrium expression for the ion pairing between ferrocenium and two different anions, *Y* and *Z*, has previously been derived (eq 3):[30]

$$E_p = E_p' - \frac{RT}{zF}\ln(K_{eff}[Y]) \quad (3)$$

where E_p is the peak potential at which half of the ferrocene has oxidized, E_p' is the E_p when ferrocenium is only in the presence of anion Z, R is the gas constant, T is the temperature, z is the number of electrons transferred in the redox reaction, F is Faraday's constant, K_{eff} is the effective formation constant for the single dominant ferrocenium-Y ion pair, and $[Y]$ is the concentration of anion Y in the solution. In the case of this experiment, Y corresponds to the anionic methacrylate group on the ferrocene copolymer, and Z corresponds to the perchlorate anion. It should be noted that although eq 3 was initially derived for the interaction of free anions in solution with surface-tethered ferrocene moieties,[30] it is assumed to be applicable in this scenario because previous homogeneous electrochemical studies of dissolved ferrocene-containing polyelectrolytes have also reported the adsorption of these redox-active polymers onto the electrode interface.[48,49] The amount of negatively charged MAA groups present in the system depends on the pH of the environment and can be described by rearranging eq 2 (eq 4):

$$[Y] = \left(\frac{[A^-]}{[HA] + [A^-]}\right)([HA] + [A^-]) = y_{A-}[HA]_{total} = \frac{[HA]_{total}}{10^{pK_a - pH} + 1} \quad (4)$$

where $[HA]_{total}$ is the total concentration of acid present as either HA or A^- and y_{A-} is the mole fraction of $[HA]_{total}$ present in the dissociated anionic state. Substitution of eq 4 into eq 3 connects the peak potential to the pH of the solution (eq 5):

$$E_p = E_p' - \frac{RT}{zF}\ln\left(K_{eff}\frac{[HA]_{total}}{10^{pK_a - pH} + 1}\right) \quad (5)$$

For pH $\ll$ pK_a, eq 5 can be approximately simplified to obtain a final relationship between E_p and pH (eq 6):

$$E_p \approx E_p' - \frac{RT}{zF}\left(\ln(K_{eff}[HA]_{total}) - \left(\frac{pK_a - pH}{\log_{10} e}\right)\right) \quad (6)$$

To complete the analysis, the experimental redox half potentials, $E_{1/2}$, of cyclic voltammograms of P($VFc_{0.05}$-*co*-$MA_{0.95}$) in solutions with apparent pH < 5 (pK_a of MAA = 4.86) were collected for use in place of E_p and subsequently seen to decrease with increases in apparent pH. Qualitatively, this trend followed the negative correlations predicted by eq 6, as well as that of the pH-dependent proportion of undissociated MAA within the polymer, $[HA]/([HA] + [A^-])$, as determined from eq 2 using pK_a of MAA = 4.86 (Figure 3c). The experiments were also repeated with molecular ferrocene in the form of a ferrocenium salt, which revealed negligible variation in the $E_{1/2}$ of the redox signal across the same pH range and confirmed that the observed trend for P($VFc_{0.05}$-*co*-$MA_{0.95}$) was not a result of increased hydroxide anion concentration with apparent pH. As well, the initial plateau observed for the $E_{1/2}$ of P($VFc_{0.05}$-*co*-$MA_{0.95}$) at low apparent pH values has been reported to be expected for homogeneous proton-consuming redox couples in permselective coatings.[43] Density functional theory (DFT) calculations for various ferrocenium-anion ion pairs have suggested that selective redox-enhanced hydrogen bonding occurs between the cyclopentadienyl ring of ferrocenium and carboxylate anions.[23] This interaction has also been supported experimentally via two separate previous studies that revealed that ferrocene moieties in the presence of only perchlorate anions experienced increasingly negative shifts in their reduction potential as formate anions were introduced to the solution at higher and higher concentrations, an observation that is consistent with the notion of increased ease of ferrocene oxidation.[22,23] Prior literature regarding ferrocene-labeled poly(acrylic acid) and mixed acid-ferrocene self-assembled monolayers also ascribed its more negative reduction potential observed under basic conditions to ferrocenium stabilization via intramolecular/interchain interaction with the higher amount of dissociated carboxylate moieties[48,50] and further suggested that charge propagation is less facile at high pH because the restricted motion of the polymer chains due to electrostatic repulsion between the charged acid groups hinders electron hopping between ferrocene sites.[48]

In the second framework, only the acid dissociation property of the comonomer in the ferrocene polyelectrolyte is considered. This alternative mechanism can be formulated by assuming that the polyelectrolyte undergoes a unique acid dissociation event when its redox moieties are in the neutral ferrocene state, and another when they are in the oxidized ferrocenium state. Such a Nernstian relation has previously been developed for the ferrocene carboxylic acid molecule, FcCOOH (eq 7):[65]

$$E_{1/2} = E^0\left(\frac{FcCOOH}{Fc^+COOH}\right) - \frac{RT}{zF}\ln\frac{K_a\left(\frac{Fc^+COOH}{Fc^+COO^-}\right) + [H^+]}{K_a\left(\frac{FcCOOH}{FcCOO^-}\right) + [H^+]} \quad (7)$$

where E^0 is the standard redox potential of the redox couple, $FcCOO^-$ is the conjugate base of FcCOOH, Fc^+COOH is ferrocenium carboxylic acid, and Fc^+COO^- is the conjugate base of Fc^+COOH. A nonlinear fit of the P($VFc_{0.05}$-*co*-$MA_{0.95}$) data in Figure 3c to eq 7 revealed decent agreement between the experimental and fitted pH-dependent redox potentials of the ferrocene methacrylate copolymers (Figure 3d). Specifically, the model fitting yielded estimates of E^0 = 0.26 V vs Ag/AgCl, p$K_a(Fc^+)$ = 3.21, and pK_a(Fc) = 4.07, with the latter pK_a corresponding to the previously reported value of 4.20,[66] and the trend of p$K_a(Fc^+)$ < pK_a(Fc) matching the one obtained for FcCOOH in an earlier study.[65]

The pH-dependent electrochemical reduction potential of the P($VFc_{0.05}$-*co*-$MA_{0.95}$) species is noteworthy because it is a designed property imparted by the inclusion of weak acid moieties within the polymer. Traditionally, the variation of redox potential with pH is a characteristic exhibited by the quinone class of compounds and is often described in this context using the archetypal redox couple (eq 8):[67]

$$Q + ne^- + mH^+ \leftrightarrow (QH_m)^{m-n} \quad (8)$$

where Q is the oxidized quinone, $(QH_m)^{m-n}$ is the reduced quinone, and n and m are coefficients that depend on the solution pH. Although the reducing redox properties of quinones lie innately with their reception of electrons and hydrogen ions in protic solutions, the ferrocene polyelectrolyte is also able to exhibit a pH-mediated redox effect without direct electrochemical reaction with protons. However, it was seen that the P($VFc_{0.05}$-*co*-$MA_{0.95}$) response did not follow the predicted slope of −59 mV/pH unit for a one-electron transfer reaction as described in eqs 5 and 6. A plausible explanation for this observation may be the quasireversible behavior exhibited

by P($VFc_{0.02}$-*co*-$MA_{0.98}$) and P($VFc_{0.05}$-*co*-$MA_{0.95}$) under the selected experimental conditions as evidenced by the peak-to-peak separations of their oxidation and reduction peaks (Figure 3a), which were larger than the characteristic ca. 57 mV value for a reversible one-electron system at 25 °C.[68] Furthermore, water splitting reactions and the unbuffered nature of the solution can give rise to pH differences between the bulk solution and the electrode interface. The latter phenomenon results in nonequilibrium conditions because the required migration of protons from the bulk solution to the electrode proceeds less quickly than electron transfer for the redox reaction,[65] and in the case of quinones, has been shown to affect their electroactivity by causing drastic deviations from the expected trend of $-m/n$ 59 mV/pH unit as predicted by eq 8 for buffered solutions. In fact, previous electrochemical experiments carried out for 2-anthraquinone sulfonate in unbuffered solutions revealed that its $E_{1/2}$ values reduced with increasing pH at a much lower rate of ca. 10 mV/pH unit in the proximity of its second acid dissociation constant,[67] which agrees more closely with the magnitude of the slope observed in Figure 3c. Correspondingly, similar pH experiments performed on homogeneous redox-active species such as ferrocenylcarboxylic acids and $[Ru(bpy)_2(2\text{-}CHOpy)]^{2+}$ were also observed to have been conducted under buffered conditions.[39,65] Additionally, it is predicted that the random nature of the copolymer, in conjunction with the low proportion of VFc within the polymer, would also hinder the ability of each and every one of the deprotonated MAA groups to effectively interact with all of the ferrocenium moieties, thus potentially manifesting as a smaller response in redox potential with pH.

Previous findings from pH studies of heterogeneously functionalized redox-active species have been observed to share similarities with the aforementioned homogeneous results. Specifically, osmium-containing polyelectrolytes,[41] ferrocene-containing polyelectrolytes,[47,51] redox-active polyelectrolyte film models,[45] and polyelectrolyte layers with impregnated or bonded redox-active species[40,43] have displayed analogous decreases in peak currents or redox potential with increases in pH in the range of the expected pK_a of their pH-sensitive components. As such, experiments on the ferrocene polyelectrolytes in a heterogeneous fashion may lead to further insight into their pH-dependent electroactive behavior.

Heterogeneous Redox Activity. As the individual presence of non-redox-active acid moieties on an electrode can result in pH-dependent capacitances,[69] it naturally follows that the interaction between electroactive and electro-inactive species affixed at an electrochemical interface is also of interest. To investigate this, P(VFc_{1-m}-*co*-X_m)-CNT electrodes were subjected to characterization using 500 mM sodium perchlorate solutions of varying pH values prepared from a modified version of the Britton–Robinson buffer system. CV experiments with P(VFc-*co*-MA)-CNT revealed that its electrode pseudocapacitance resulting from oxidizing ferrocene units was roughly constant at ca. 200 to 240 F/g VFc regardless of pH, suggesting that in a heterogeneous framework, there is reduced hindering of ferrocene activation from the anionic methacrylic acid groups (Figure 4a and Figure S14, SI). It was also observed that the capacity of the heterogeneously functionalized P(VFc-*co*-MA) copolymer was maintained relatively well over repeated and rigorous electrochemical cycling at fast 0.1 V/s scan rates, with the

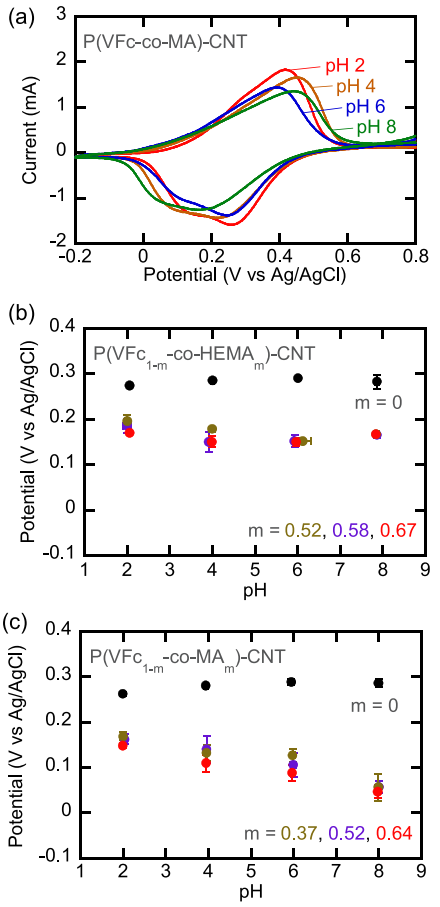

Figure 4. (a) Representative heterogeneous CVs of P(VFc-*co*-MA)-CNT after two cycles at 0.01 V/s in buffered aqueous solutions with differing pH values. Electrochemical potentials of (b) P(VFc_{1-m}-*co*-MA_m)-CNT and (c) P(VFc_{1-m}-*co*-$HEMA_m$)-CNT at different buffered pH values, obtained from chronopotentiometry experiments after 100 s at 2 μA (ca. 0.02 A/m^2). The aqueous solutions of varying pH values were prepared using a modified version of the Britton–Robinson buffer system and 0.5 M $NaClO_4$ supporting electrolyte.

lower retention in higher pH solutions attributed to its heightened hydrophilicity and hence, stronger attraction to the bulk aqueous phase under these conditions (Figure S15, SI). Contrastingly, it is interesting to note that heterogeneously tethered osmium bipyridine polymers displayed decreasing pseudocapacitances with increasing pH, a phenomenon which was ascribed to the loss of the quasidiffusional flexibility of the polymer chains due to their shrinking and collapse from pyridine deprotonation in a basic environment.[41,42]

Specific electrode potentials were also determined under kinetic conditions of chronopotentiometry over a short duration of only 100 s to emulate more realistic operating circumstances as opposed to using equilibrium-based cyclic voltammetric testing. The resulting chronopotentiometric studies showed that the measured potential of the PVFc-CNT homopolymer composite did not change significantly with pH, which was expected because the generation of positive charge through ferrocenium formation is redox-mediated. However, when performed on the ferrocene copolymers, the chronopotentiometry experiments revealed that with increasing pH values, the redox potentials of the P(VFc_{1-m}-*co*-$HEMA_m$)-CNT electrodes remained constant (Figure 4b), corroborating the previous observation that the

reduction potential of homogeneous ferrocenium was effectively unaffected by hydroxide concentration (Figure 3c), whereas P(VFc$_{1-m}$-*co*-MA$_m$)-CNT exhibited decreasing potentials spanning a range of ca. 100 to 110 mV between pH values of ca. 2 and 8 (Figure 4c). The observed trends were consistent across different nonzero mole fractions of both nonredox-active comonomers without discernable difference in the nature of the correlation and can be ascribed to the propensity of the inert comonomer to become charged. In the case of P(VFc$_{1-m}$-*co*-MA$_m$)-CNT, the observed redox behavior can be attributed to Donnan potential differences between the polyelectrolyte interface and the solution,[41,43,45] a phenomenon that has previously been leveraged for ion permselectivity.[43,44,47,60,61] The Donnan potential can be expressed as (eq 9):[44,61,70]

$$\Delta\phi_D = E_{1/2} - E^0 = \frac{RT}{F}\ln\left[\frac{C_F + (C_F^2 + 4C_S^2)^{1/2}}{2C_S}\right] \quad (9)$$

where $\Delta\phi_D$ is the Donnan potential, C_F is the concentration of fixed charge sites, and C_S is the electrolyte concentration. From eq 9, it can be observed that for any nonzero electrolyte concentration ($C_S > 0$) and nonzero concentration of fixed negative charge sites ($C_F < 0$), the Donnan potential, $\Delta\phi_D$, will be negative. At a constant value of C_S, an increasingly negative value of C_F will accordingly result in an increasingly negative value of $\Delta\phi_D$. For the ferrocene polyelectrolytes, this would mean that at a higher solution pH where more of the acidic groups are deprotonated to their negatively charged forms, the value of C_F would become more negative, resulting in a lower observed redox potential and thus qualitatively corresponding with the responses previously observed for P(VFc-*co*-MA)-CNT and P(VFc-*co*-SS)-CNT in solutions of varying basicities (Figures 2b and 4c, and Figure S11, SI). Among other assumptions, if the effects of the solution ionic strength and the redox state of the ferrocene moieties on C_F may be neglected,[44,61,70] eq 9 can be applied for the quantitative estimation of C_S at a given pH value. Using the data in Figure 4a with the additional assumptions of $E^0 = E_{1/2}$(pH = 2) and C_S = 0.5 M, eq 9 was solved nonlinearly to yield negative C_S values that increased in magnitude with solution pH (Table S3, SI).

From these results, it can be surmised that the overall electrochemical potential of the electrode is influenced by both the innate Faradaic reaction of the ferrocene redox moiety and the acidity of the nonredox comonomer. To study this further, sequential chronopotentiometry experiments at increasing currents were performed using P(VFc-*co*-*X*)-CNT electrodes at different pH values. At an applied current of 2 μA (ca. 0.02 A/m^2), the total potential range from pH ca. 2 to 8 afforded by P(VFc-*co*-SS)-CNT was 170 mV, followed by that of 89 mV from P(VFc-*co*-MA)-CNT (Figure 5a). When the current was subsequently raised to 10 μA (ca. 0.1 A/m^2) and 50 μA (ca. 0.5 A/m^2), these values changed to 112 and 92 mV, (Figure 5b) and 88 and 77 mV (Figure 5c), respectively. As with the previous chronopotentiometry experiments, the reduction in electrochemical potential with increase in pH was only seen with polymers containing acidic comonomers, and minimal differences in potential were noted for the nonacidic PVFc-CNT and P(VFc-*co*-HEMA)-CNT materials. However, it was observed that in general, the potentials of all polymers except the PVFc homopolymer increased with elevated current density and tended progressively closer to the constant

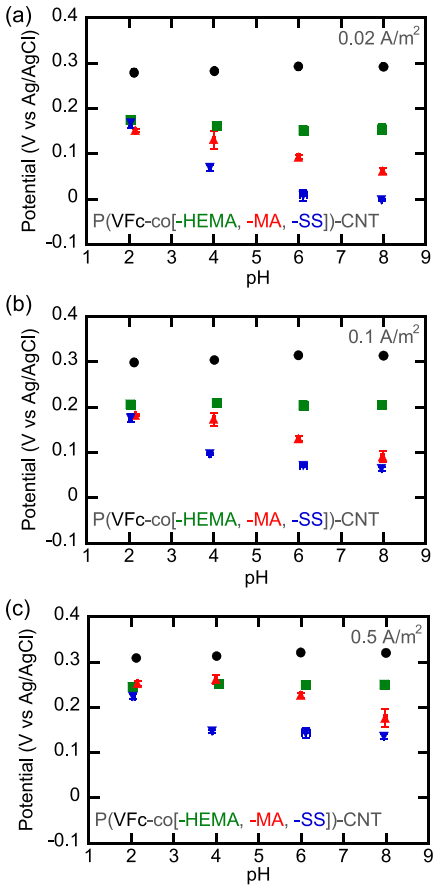

Figure 5. Electrochemical potentials of P(VFc-*co*-*X*)-CNT at different buffered pH values, obtained from continuous and sequential chronopotentiometry experiments starting from (a) 2 μA (ca. 0.02 A/m^2), followed by (b) 10 μA (ca. 0.1 A/m^2), and lastly (c) 50 μA (ca. 0.5 A/m^2). Electrochemical values were taken after 100 s, the duration of chronopotentiometry applied at each current step. The aqueous solutions of varying pH values were prepared using a modified version of the Britton−Robinson buffer system and 0.5 M $NaClO_4$ supporting electrolyte.

PVFc-CNT potential when greater currents were applied. These findings suggest that the effect of acidic anionic groups on the potential dominates at low currents, whereas Faradaic ferrocene oxidation governs the potential at high currents. Specifically, at sufficiently large currents, it is expected that the decline in electrochemical potential from Donnan effects afforded by the charged species can no longer offset the increase in electrode potential resulting from the heightened oxidation of ferrocene units to sustain the passed current.

Electrochemical Separation of Transition Metal Oxyanions. The application of the ferrocene copolymers to ion separation was studied using the PVFc and P(VFc$_{0.63}$-*co*-MA$_{0.37}$) polyelectrolytes in the presence of heavy metal oxyanions (HMOAs). The m = 0.37 variation of the P(VFc$_{1-m}$-*co*-MA$_m$) motif was selected to ensure a strong redox-active response as a result of the heightened proportion of VFc groups within the overall polymer, which was subsequently confirmed through the distinct oxidation and reduction peaks corresponding to the ferrocene moieties (Figure S16, SI). Ferrocene has previously been reported to exhibit selective affinities for vanadium and chromium oxyanions over competing electrolyte species,[24,27] and can remove such anions via the redox-mediated formation of

surface-attached ferrocenium-anion complexes (Figure 6a).[24,25,27,33] As such, these strongly binding oxyanions were

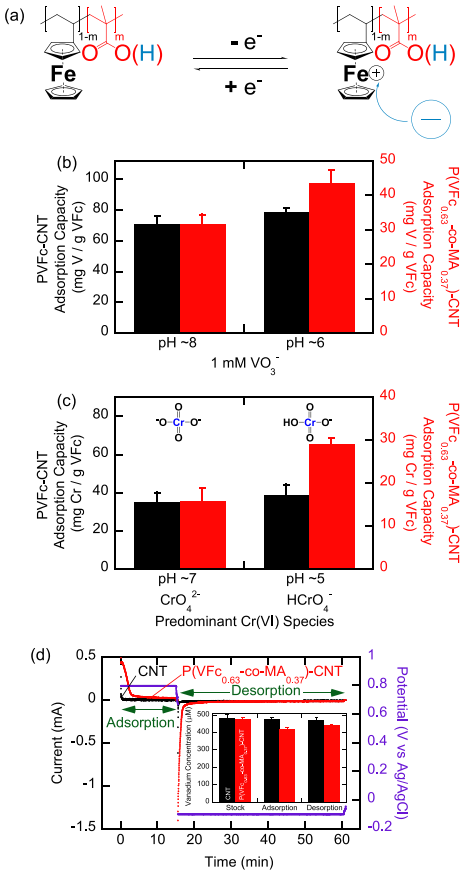

Figure 6. (a) Schematic depicting redox-mediated reversible P(VFc-*co*-MA)-anion complex formation. Electrosorption capacities of PVFc-CNT and P($VFc_{0.63}$-*co*-$MA_{0.37}$)-CNT for (b) vanadium from 1 mM $NaVO_3$ (10 mM $NaClO_4$ supporting electrolyte) solutions after 30 min at 0.8 V vs Ag/AgCl at different pH values and (c) chromium from 500 μM $Na_2Cr_2O_7$ and 1 mM Na_2CrO_4 (10 mM $NaClO_4$ supporting electrolyte in both cases) solutions after 30 min at 0.8 V vs Ag/AgCl. (d) Inset: concentrations of vanadium in a 500 μM $NaVO_3$ solution with 10 mM $NaClO_4$ supporting electrolyte before electrosorption, after adsorption for 15 min at 0.8 V vs Ag/AgCl with P($VFc_{0.63}$-*co*-$MA_{0.37}$)-CNT and CNT electrodes, and after subsequent desorption for 45 min at −0.1 V vs Ag/AgCl. The P($VFc_{0.63}$-*co*-$MA_{0.37}$)-CNT and CNT electrodes were left at open-circuit voltage for 30 s after both the adsorption and desorption steps for the purpose of sample collection. Error bars were calculated using the % relative standard deviation (RSD) values for ICP-OES vanadium concentration measurements of the extracted samples. Outset: chronoamperometric traces of the sequenced adsorption and desorption experiments as described in the inset for the P($VFc_{0.63}$-*co*-$MA_{0.37}$)-CNT and CNT electrodes.

selected as the analytes in this study with the intention of allowing any effects of the non-redox-active anionic moiety on the electrosorption capacity of the overall ferrocene polymer to be more clearly observed.

Pentavalent vanadium in the form of metavanandate oxyanions was subjected to electrosorption by PVFc-CNT and P($VFc_{0.63}$-*co*-$MA_{0.37}$)-CNT at the as-made solution pH of 1 mM $NaVO_3$ (pH ca. 6), and at a higher pH value manually adjusted with 0.1 M NaOH (pH ca. 8) (Figure 6b). This experimental pH range was selected because vanadium is expected to speciate as an anion only above a pH of around 3,[27,71] thus deconvoluting the effect of the electrostatic charge of vanadium from that of solution basicity in regard to separation performance. Separation results after 30 min at 0.8 V vs Ag/AgCl with 10 mM $NaClO_4$ supporting electrolyte revealed an approximately 50% increase in adsorption when PVFc-CNT was used instead of P($VFc_{0.63}$-*co*-$MA_{0.37}$)-CNT. The contrast in vanadium recovery can be attributed to the presence of the pH-dependent MAA moieties in P($VFc_{0.63}$-*co*-$MA_{0.37}$), which were expected to be already more than 90% deprotonated at pH ca. 6 and likely repelled negatively charged ions from approaching the ferrocene polymer electrode. Correspondingly, it was observed that a decrease in solution pH was also associated with a ca. 35% improvement in the P($VFc_{0.63}$-*co*-$MA_{0.37}$)-CNT sorption capacity from 32 to 43 mg V/g VFc. However, as the quantity of vanadium separated by PVFc-CNT also experienced a modest ca. 10% rise from 70 to 79 mg V/g VFc alongside a lowering in pH, it is also possible that the change in the vanadium uptake of P($VFc_{0.63}$-*co*-$MA_{0.37}$)-CNT with a higher solution basicity was partially influenced by the fouling of the ferrocenium sites from an increased presence of strongly nucleophilic hydroxide anions.[19]

To further probe the electrosorption properties of P($VFc_{0.63}$-*co*-$MA_{0.37}$)-CNT, chromium HMOAs were investigated by carrying out electrochemical separation experiments with PVFc-CNT and P($VFc_{0.63}$-*co*-$MA_{0.37}$)-CNT electrodes in aqueous solutions prepared from Na_2CrO_4 and $Na_2Cr_2O_7$ salts at a concentration of 1 mM Cr and with 10 mM $NaClO_4$ supporting electrolyte (Figure 6c). As in the case of metavanandate sorption, a difference in separation performance was observed in the Na_2CrO_4 solution, with chromium adsorption quantities of 35 and 16 mg Cr/g VFc yielded by PVFc-CNT and P($VFc_{0.63}$-*co*-$MA_{0.37}$)-CNT, respectively. However, in the $Na_2Cr_2O_7$ solution, P($VFc_{0.63}$-*co*-$MA_{0.37}$)-CNT separated 29 mg Cr/g VFc, almost double its removal amount in the Na_2CrO_4 solution and only slightly lower than the value of 39 mg Cr/g VFc achieved with PVFc-CNT. pH measurements of both solutions yielded readings of 7.2 for Na_2CrO_4 and 4.9 for $Na_2Cr_2O_7$. From these values, the predominant hexavalent chromium species for the Na_2CrO_4 and $Na_2Cr_2O_7$ solutions are speculated to be CrO_4^{2-} and $HCrO_4^-$, respectively.[72] The affinity of the ferrocenium molecule for these two oxyanions did not appear to vary appreciably as per the very similar amounts of chromium removed by PVFc-CNT in each solution, an observation that was further corroborated by results from a previous study that reported comparable binding energies of ca. 1 kcal/mol from DFT calculations for both Fc^+-$HCrO_4^-$ and Fc^+-CrO_4^{2-}.[24] Additionally, P($VFc_{0.63}$-*co*-$MA_{0.37}$) was expected to transition from being only 58% deprotonated to an almost fully (>99%) deprotonated state between pH 5 and 7, resulting in a much greater amount of negatively charged groups present at the electrode interface when in the Na_2CrO_4 solution. As such, the dissimilarity in the uptake capacities of P($VFc_{0.63}$-*co*-$MA_{0.37}$)-CNT for different chromium species can once again be ascribed to its pH-dependent MAA moieties. It is presumed that the decline in adsorption due to electrostatic repulsion intensifies in increasingly basic environments as more MAA groups deprotonate to their anionic forms and not because of a lower amount of ferrocene oxidation, as partially supported by the observation that the amounts of charge passed through P($VFc_{0.63}$-*co*-$MA_{0.37}$)-CNT during the electrosorption experiments at both pH values were nearly the same (Figure S17,

SI). As $HCrO_4^-$ and CrO_4^{2-} exist and speciate in water at unique pH ranges because of innate chemical equilibrium relationships, the MAA species effectively impart P($VFc_{0.63}$-*co*-$MA_{0.37}$) with a higher selectivity for the more acidic $HCrO_4^-$ over the more basic CrO_4^{2-}. In other words, although the $PVFc^+$-CNT homopolyelectrolyte can achieve strong overall separation performance for both chromium species, the P($VFc_{0.63}^+$-*co*-$MA_{0.37}^-$)-CNT polyelectrolyte provides further subtlety in separation in terms of anion differentiation, enabling a proportionally larger ca. twofold difference in chromium anion uptake capacity at lower pH values.

Finally, the redox-active properties of P($VFc_{0.63}$-*co*-$MA_{0.37}$) were further challenged in a sequenced experiment at a lower analyte concentration. Specifically, P($VFc_{0.63}$-*co*-$MA_{0.37}$)-CNT was placed in a 500 μM $NaVO_3$ solution and subjected to an oxidation potential of 0.8 V vs Ag/AgCl for 15 min for vanadium adsorption, followed by a reduction potential of −0.1 V vs Ag/AgCl for 45 min for subsequent vanadium desorption, with the same experiment also repeated using a control electrode containing only CNT (Figure 6d). Even at this reduced concentration, P($VFc_{0.63}$-*co*-$MA_{0.37}$)-CNT was able to remove vanadium at a capacity of 22.4 mg V/g VFc or 4.5 μg V (12.3% of the initial amount in the 500 μM solution), which was almost one order of magnitude larger than that of 0.6 μg V (1.6% of the initial amount in the 500 μM solution) obtained with the CNT control electrode. Furthermore, the P($VFc_{0.63}$-*co*-$MA_{0.37}$)-CNT electrode exhibited electrochemical reversibility in its separation process, which was observed by tracking the balance of the total number of moles of vanadium from inductively coupled plasma-optical emission spectroscopy (ICP-OES) measurements of the vanadium concentrations before adsorption, after adsorption, and after desorption, as well as taking into consideration the moles of vanadium present in the extracted samples themselves. In contrast to the experiment with the CNT electrode, a clear increase in the amount of solution phase vanadium present at the end of the electrodesorption stage compared to the amount at its start was observed. This difference was attributed to the release of the vanadium initially electrosorbed during the adsorption stage and corresponded numerically to a vanadium recovery amount of 41.6%, which is appreciable considering the relatively mild potential used to reverse the adsorption and the presence of a concentration gradient for vanadium disfavoring its mass transfer from the electrode back into the solution. Furthermore, in a previous work regarding continuous electrochemical vanadium removal with PVFc-CNT in a flow cell system, it has been reported that electrodesorption under certain conditions can result in the formation of vanadium cations, which may subsequently readsorb onto the PVFc-CNT electrode.[27] Swollen polyelectrolyte layers may also result in the generation of Donnan domains possessing confined counterions within the polymer coating.[61] However, although the aforementioned conditions were selected to challenge the system as they are more representative of realistic process conditions for material regeneration, ferrocene materials have nevertheless been previously shown to possess robust reversible properties,[19,22,24−27] and it is thus fully expected that complete reversibility can be achieved with additional improvements such as the use of a clean solution devoid of analyte for desorption, the introduction of flow to the process, as well as the optimization of operating parameters like electrodesorption potential and duration.

CONCLUSIONS

A series of hydrophilic redox-active ferrocene polymers was developed for the investigation of their pH and electrochemical properties in aqueous media. Ferrocene macromolecules containing acid moieties possessed zwitterionic properties as a result of acid dissociation and electrochemical oxidation, and their pH-sensitive electrochemical behavior was studied in both the solution state as a dissolved species, as well as on electrode interfaces as ferrocene copolymer-carbon nanotube composites. The zwitterionicity of these materials was subsequently applied to the electrochemical separation of transition metals based on solution pH, and produced an almost doubled affinity toward chromium in its acidic hydrogen chromate state compared to its more basic chromate form when methacrylic acid moieties were incorporated into the ferrocene polymer. The imparting of pH-responsive properties to an innately pH-independent redox-active species is especially interesting and highly applicable to the future development of water-based stimuli-responsive technologies for molecular targeting and separation.

AUTHOR INFORMATION

Corresponding Author

T. **Alan Hatton** − *Department of Chemical Engineering, Massachusetts Institute of Technology, Cambridge, Massachusetts 02139, United States of America;* orcid.org/0000-0002-4558-245X; Email: tahatton@mit.edu

Authors

Kai-Jher Tan − *Department of Chemical Engineering, Massachusetts Institute of Technology, Cambridge, Massachusetts 02139, United States of America;* orcid.org/0000-0001-7705-3774

Satoshi Morikawa − *Department of Chemical Engineering, Massachusetts Institute of Technology, Cambridge, Massachusetts 02139, United States of America;* Present Address: Household Product Research Laboratory, Kao Corporation, 1334 Minato, Wakayama-shi, Wakayama 640-8580, Japan

Nil Ozbek − *Department of Chemical Engineering, Massachusetts Institute of Technology, Cambridge, Massachusetts 02139, United States of America; Department of Chemical Engineering, Faculty of Chemical and Metallurgical Engineering, Istanbul Technical University, 34469 Istanbul, Turkey*

Magdalena Lenz − *Department of Chemical Engineering, Massachusetts Institute of Technology, Cambridge, Massachusetts 02139, United States of America;* Present Address: Institute of Functional Interfaces (IFG), Karlsruhe Institute of Technology, Hermann-von-Helmholtz-Platz 1, Eggenstein-Leopoldshafen, Baden-Württemberg 76344, Germany

Carsten-René Arlt − *Department of Chemical Engineering, Massachusetts Institute of Technology, Cambridge,*

Massachusetts 02139, United States of America; Present Address: Institute of Functional Interfaces (IFG), Karlsruhe Institute of Technology, Hermann-von-Helmholtz-Platz 1, Eggenstein-Leopoldshafen, Baden-Württemberg 76344, Germany

André Tschöpe − *Department of Chemical Engineering, Massachusetts Institute of Technology, Cambridge, Massachusetts 02139, United States of America;* Present Address: Institute of Functional Interfaces (IFG), Karlsruhe Institute of Technology, Hermann-von-Helmholtz-Platz 1, Eggenstein-Leopoldshafen, Baden-Württemberg 76344, Germany

Matthias Franzreb − *Institute of Functional Interfaces (IFG), Karlsruhe Institute of Technology, Eggenstein-Leopoldshafen, Baden-Württemberg 76344, Germany;* orcid.org/0000-0003-3586-4215

Author Contributions

K.-J.T. and T.A.H. conceived the project concept and were involved in all scientific considerations. K.-J.T. wrote the manuscript, with revisions and discussions from M.F. and T.A.H. K.-J.T., S.M., N.O., M.L., C.-R.A., and A.T. performed the experiments.

Funding

K.-J.T. was supported by a Natural Sciences and Engineering Research Council of Canada (NSERC) postgraduate doctoral scholarship (PGS D). M.L., C.-R.A., and A.T. were funded by the Karlsruhe House of Young Scientists (KHYS).

Notes

The authors declare no competing financial interest.

ACKNOWLEDGMENTS

This work made use of the Department of Chemistry Instrumentation Facility (DCIF) at the Massachusetts Institute of Technology, as well as the Center for Nanoscale Systems (CNS) at Harvard University (supported by the National Science Foundation under Award No. 1541959). The authors gratefully acknowledge Dr. Yayuan Liu for help with preliminary XPS measurements and Dr. Seoni Kim for assistance with certain ICP-OES experiments.

ABBREVIATIONS

Fc, ferrocene; VFc, vinylferrocene; PVFc, poly(vinylferrocene); MA, methacrylate; MAA, methacrylic acid; SS, 4-styrene sulfonate; HEMA, 2-hydroxyethyl methacrylate; CNT, carbon nanotube; HMOA, heavy metal oxyanion

REFERENCES

(1) Kim, J.; Kim, J. H.; Ariga, K. Redox-Active Polymers for Energy Storage Nanoarchitectonics. *Joule* **2017**, *1*, 739−768.

(2) Beer, P. D.; Gale, P. A.; Chen, G. Z. Mechanisms of electrochemical recognition of cations, anions and neutral guest species by redox-active receptor molecules. *Coord. Chem. Rev.* **1999**, *185-186*, 3−36.

(3) Luca, O. R.; Crabtree, R. H. Redox-active ligands in catalysis. *Chem. Soc. Rev.* **2013**, *42*, 1440−1459.

(4) Tan, K.-J.; Hatton, T. A. Electrochemically Mediated Sustainable Separations in Water. In *Sustainable Separation Engineering*; 1 ed.; Szekely, G., Zhao, D. Eds.; Wiley Online Books, Vol. 1; John Wiley & Sons Ltd., 2022; pp. 1−62.

(5) Nam, D.-H.; Lumley, M. A.; Choi, K.-S. Electrochemical Redox Cells Capable of Desalination and Energy Storage: Addressing Challenges of the Water−Energy Nexus. *ACS Energy Lett.* **2021**, *6*, 1034−1044.

(6) Kaifer, A. E. Interplay between Molecular Recognition and Redox Chemistry. *Acc. Chem. Res.* **1999**, *32*, 62−71.

(7) Bakker, E.; Telting-Diaz, M. Electrochemical Sensors. *Anal. Chem.* **2002**, *74*, 2781−2800.

(8) Manjakkal, L.; Szwagierczak, D.; Dahiya, R. Metal oxides based electrochemical pH sensors: Current progress and future perspectives. *Prog. Mater. Sci.* **2020**, *109*, No. 100635.

(9) Capannesi, C.; Palchetti, I.; Mascini, M.; Parenti, A. Electrochemical sensor and biosensor for polyphenols detection in olive oils. *Food Chem.* **2000**, *71*, 553−562.

(10) Chen, F.; Leong, Z. Y.; Yang, H. Y. An aqueous rechargeable chloride ion battery. *Energy Storage Mater.* **2017**, *7*, 189−194.

(11) Lilga, M. A.; Orth, R. J.; Sukamto, J. P. H.; Haight, S. M.; Schwartz, D. T. Metal ion separations using electrically switched ion exchange. *Sep. Purif. Technol.* **1997**, *11*, 147−158.

(12) Sukamto, J. P. H.; Rassat, S. D.; Orth, R. J.; Lilga, M. A. Electrochemical Ion Exchange. In *Encyclopedia of Separation Science*; Wilson, I. D. Ed.; Academic Press, 2000.

(13) (a) Kim, K.; Baldaguez Medina, P.; Elbert, J.; Kayiwa, E.; Cusick, R. D.; Men, Y.; Su, X. Molecular Tuning of Redox-Copolymers for Selective Electrochemical Remediation. *Adv. Funct. Mater.* **2020**, *30*, 2004635. (b) Kim, K.; Cotty, S.; Elbert, J.; Chen, R.; Hou, C.-H.; Su, X. Asymmetric Redox-Polymer Interfaces for Electrochemical Reactive Separations: Synergistic Capture and Conversion of Arsenic. *Adv. Mater.* **2020**, *32*, 1906877.

(14) Piletsky, S. A.; Turner, A. P. F. Electrochemical Sensors Based on Molecularly Imprinted Polymers. *Electroanalysis* **2002**, *14*, 317−323.

(15) (a) Karyakin, A. A. Prussian Blue and Its Analogues: Electrochemistry and Analytical Applications. *Electroanalysis* **2001**, *13*, 813−819. (b) Liu, L.; Zhou, Y.; Liu, S.; Xu, M. The Applications of Metal−Organic Frameworks in Electrochemical Sensors. *ChemElectroChem* **2018**, *5*, 6−19.

(16) Miasik, J. J.; Hooper, A.; Tofield, B. C. Conducting polymer gas sensors. *J. Chem. Soc., Faraday Trans. 1* **1986**, *82*, 1117−1126.

(17) (a) Wen, Q.; Liu, L.; Yang, Q.; Lv, F.; Wang, S. Dopamine-Modified Cationic Conjugated Polymer as a New Platform for pH Sensing and Autophagy Imaging. *Adv. Funct. Mater.* **2013**, *23*, 764−769. (b) Liu, Y.; Ye, H.-Z.; Diederichsen, K. M.; Van Voorhis, T.; Hatton, T. A. Electrochemically mediated carbon dioxide separation with quinone chemistry in salt-concentrated aqueous media. *Nat. Commun.* **2020**, *11*, 2278. (c) Hemmatifar, A.; Kang, J. S.; Ozbek, N.; Tan, K.-J.; Hatton, T. A. Electrochemically Mediated Direct CO2 Capture by a Stackable Bipolar Cell. *ChemSusChem* **2022**, *15*, e202102533.

(18) Holliday, B. J.; Stanford, T. B.; Swager, T. M. Chemoresistive Gas-Phase Nitric Oxide Sensing with Cobalt-Containing Conducting Metallopolymers. *Chem. Mater.* **2006**, *18*, 5649−5651.

(19) Su, X.; Tan, K.-J.; Elbert, J.; Rüttiger, C.; Gallei, M.; Jamison, T. F.; Hatton, T. A. Asymmetric Faradaic systems for selective electrochemical separations. *Energy Environ. Sci.* **2017**, *10*, 1272−1283.

(20) Sun, R.; Wang, L.; Yu, H.; Abdin, Z.-U.; Chen, Y.; Huang, J.; Tong, R. Molecular Recognition and Sensing Based on Ferrocene Derivatives and Ferrocene-Based Polymers. *Organometallics* **2014**, *33*, 4560−4573.

(21) Saleem, M.; Yu, H.; Wang, L.; Khalid, H.; Akram, M.; Abbasi, N. M.; Huang, J. Review on synthesis of ferrocene-based redox polymers and derivatives and their application in glucose sensing. *Anal. Chim. Acta* **2015**, *876*, 9−25.

(22) Achilleos, D. S.; Hatton, T. A. Selective Molecularly Mediated Pseudocapacitive Separation of Ionic Species in Solution. *ACS Appl. Mater. Interfaces* **2016**, *8*, 32743−32753.

(23) Su, X.; Kulik, H. J.; Jamison, T. F.; Hatton, T. A. Anion-Selective Redox Electrodes: Electrochemically Mediated Separation

with Heterogeneous Organometallic Interfaces. *Adv. Funct. Mater.* **2016**, *26*, 3394−3404.
(24) Su, X.; Kushima, A.; Halliday, C.; Zhou, J.; Li, J.; Hatton, T. A. Electrochemically-mediated selective capture of heavy metal chromium and arsenic oxyanions from water. *Nat. Commun.* **2018**, *9*, 4701.
(25) Tan, K.-J.; Su, X.; Hatton, T. A. An Asymmetric Iron-Based Redox-Active System for Electrochemical Separation of Ions in Aqueous Media. *Adv. Funct. Mater.* **2020**, *30*, 1910363.
(26) He, F.; Hemmatifar, A.; Bazant, M. Z.; Hatton, T. A. Selective adsorption of organic anions in a flow cell with asymmetric redox active electrodes. *Water Res.* **2020**, *182*, No. 115963.
(27) Hemmatifar, A.; Ozbek, N.; Halliday, C.; Hatton, T. A. Electrochemical Selective Recovery of Heavy Metal Vanadium Oxyanion from Continuously Flowing Aqueous Streams. *ChemSusChem* **2020**, *13*, 3865−3874.
(28) Connelly, N. G.; Geiger, W. E. Chemical Redox Agents for Organometallic Chemistry. *Chem. Rev.* **1996**, *96*, 877−910.
(29) (a) Ju, H.; Leech, D. Effect of electrolytes on the electrochemical behaviour of 11-(ferrocenylcarbonyloxy)-undecanethiol SAMs on gold disk electrodes. *Phys. Chem. Chem. Phys.* **1999**, *1*, 1549−1554. (b) Norman, L. L.; Badia, A. Microcantilevers Modified with Ferrocene-Terminated Self-Assembled Monolayers: Effect of Molecular Structure and Electrolyte Anion on the Redox-Induced Surface Stress. *J. Phys. Chem. C* **2011**, *115*, 1985−1995. (c) Rowe, G. K.; Creager, S. E. Interfacial Solvation and Double-Layer Effects on Redox Reactions in Organized Assemblies. *J. Phys. Chem.* **1994**, *98*, 5500−5507. (d) Rudnev, A. V.; Zhumaev, U.; Utsunomiya, T.; Fan, C.; Yokota, Y.; Fukui, K.-I.; Wandlowski, T. Ferrocene-terminated alkanethiol self-assembled monolayers: An electrochemical and in situ surface-enhanced infra-red absorption spectroscopy study. *Electrochim. Acta* **2013**, *107*, 33−44. (e) Valincius, G.; Niaura, G.; Kazakevičienė, B.; Talaikytė, Z.; Kažemėkaitė, M.; Butkus, E.; Razumas, V. Anion Effect on Mediated Electron Transfer through Ferrocene-Terminated Self-Assembled Monolayers. *Langmuir* **2004**, *20*, 6631−6638. (f) Wong, R. A.; Yokota, Y.; Wakisaka, M.; Inukai, J.; Kim, Y. Probing consequences of anion-dictated electrochemistry on the electrode/monolayer/electrolyte interfacial properties. *Nat. Commun.* **2020**, *11*, 4194.
(30) Rowe, G. K.; Creager, S. E. Redox and ion-pairing thermodynamics in self-assembled monolayers. *Langmuir* **1991**, *7*, 2307−2312.
(31) (a) Gagne, R. R.; Koval, C. A.; Lisensky, G. C. Ferrocene as an internal standard for electrochemical measurements. *Inorg. Chem.* **1980**, *19*, 2854−2855. (b) Noviandri, I.; Brown, K. N.; Fleming, D. S.; Gulyas, P. T.; Lay, P. A.; Masters, A. F.; Phillips, L. The Decamethylferrocenium/Decamethylferrocene Redox Couple: A Superior Redox Standard to the Ferrocenium/Ferrocene Redox Couple for Studying Solvent Effects on the Thermodynamics of Electron Transfer. *J. Phys. Chem. B* **1999**, *103*, 6713−6722.
(32) (a) Schlindwein, W. S.; Kavvada, A.; Latham, R. J.; Linford, R. G. Electrochemical studies of poly(vinylferrocene) films in aqueous and non-aqueous electrolyte solutions. *Polym. Int.* **2000**, *49*, 953−959. (b) Inzelt, G.; Bácskai, J. Electrochemical quartz crystal microbalance study of the swelling of poly(vinylferrocene) films. *Electrochim. Acta* **1992**, *37*, 647−654. (c) Gülce, H.; Özyörük, H.; Yildiz, A. Electrochemical response of poly(vinylferrocenium)-coated Pt electrods to some anions in aqueous media. *Electroanalysis* **1995**, *7*, 178−183. (d) Jureviciute, I.; Bruckenstein, S.; Hillman, A. R. Counter-ion specific effects on charge and solvent trapping in poly(vinylferrocene) films. *J. Electroanal. Chem.* **2000**, *488*, 73−81. (e) Barbero, C.; Miras, M. C.; Calvo, E. J.; Kötz, R.; Haas, O. A Probe Beam Deflection Study of Ion Exchange at Poly(vinylferrocene) Films in Aqueous and Nonaqueous Electrolytes. *Langmuir* **2002**, *18*, 2756−2764.
(33) Tan, K.-J.; Morikawa, S.; Phillips, K. R.; Ozbek, N.; Hatton, T. A. Redox-Active Magnetic Composites for Anionic Contaminant Removal from Water. *ACS Appl. Mater. Interfaces* **2022**, *14*, 8974−8983.
(34) Arimoto, F. S.; Haven, A. C., Jr. Derivatives of Dicyclopentadienyliron1. *J. Am. Chem. Soc.* **1955**, *77*, 6295−6297.
(35) (a) Hudson, R. D. A. Ferrocene polymers: current architectures, syntheses and utility. *J. Organomet. Chem.* **2001**, *637-639*, 47−69. (b) Pietschnig, R. Polymers with pendant ferrocenes. *Chem. Soc. Rev.* **2016**, *45*, 5216−5231. (c) Gallei, M.; Rüttiger, C. Recent Trends in Metallopolymer Design: Redox-Controlled Surfaces, Porous Membranes, and Switchable Optical Materials Using Ferrocene-Containing Polymers. *Chem. − Eur. J.* **2018**, *24*, 10006−10021. (d) Tonhauser, C.; Alkan, A.; Schömer, M.; Dingels, C.; Ritz, S.; Mailänder, V.; Frey, H.; Wurm, F. R. Ferrocenyl Glycidyl Ether: A Versatile Ferrocene Monomer for Copolymerization with Ethylene Oxide to Water-Soluble, Thermoresponsive Copolymers. *Macromolecules* **2013**, *46*, 647−655. (e) Borchers, P. S.; Strumpf, M.; Friebe, C.; Nischang, I.; Hager, M. D.; Elbert, J.; Schubert, U. S. Aqueous Redox Flow Battery Suitable for High Temperature Applications Based on a Tailor-Made Ferrocene Copolymer. *Adv. Energy Mater.* **2020**, *10*, 2001825.
(36) (a) Akhoury, A.; Bromberg, L.; Hatton, T. A. Redox-Responsive Gels with Tunable Hydrophobicity for Controlled Solubilization and Release of Organics. *ACS Appl. Mater. Interfaces* **2011**, *3*, 1167−1174. (b) Baldwin, M. G.; Johnson, K. E. Free-radical polymerization of vinyl ferrocene. *J. Polym. Sci., Part A: Polym. Chem.* **1967**, *5*, 2091−2098. (c) Lai, J. C.; Rounsfell, T.; Pittman, C. U. Free-radical homopolymerization and copolymerization of vinylferrocene. *J. Polym. Sci., Part A: Polym. Chem.* **1971**, *9*, 651−662. (d) Saito, T.; Watanabe, M. Characterization of poly(vinylferrocene-co-2-hydroxyethyl methacrylate) for use as electron mediator in enzymatic glucose sensor. *React. Funct. Polym.* **1998**, *37*, 263−269. (e) Tsubokawa, N.; Abe, N.; Wei, G.; Chen, J.; Saitoh, S.; Fujiki, K. Grafting of polymers onto a carbon-fiber surface by ligand-exchange reaction of poly(vinyl ferrocene-co-vinyl monomer) with polycondensed aromatic rings of the surface. *J. Polym. Sci., Part A: Polym. Chem.* **2002**, *40*, 1868−1875. (f) Espenscheid, M. W.; Martin, C. R. Electroactive ion exchange polymers. *J. Electroanal. Chem. Interfacial Electrochem.* **1985**, *188*, 73−84. (g) Lee, M.-H.; Hong, Y. T.; Rhee, S. B. Preparation of polypyrrole doped with ferrocenic polymer dopants. *Synth. Met.* **1995**, *69*, 515−516.
(37) (a) Himuro, Y.; Takai, M.; Ishihara, K. Poly(vinylferrocene-co-2-hydroxyethyl methacrylate) mediator as immobilized enzyme membrane for the fabrication of amperometric glucose sensor. *Sens. Actuators, B* **2009**, *136*, 122−127. (b) Kuramoto, N.; Shishido, Y. Property of thermo-sensitive and redox-active poly(N-cyclopropylacrylamide-co-vinylferrocene) and poly(N-isopropylacrylamide-co-vinylferrocene). *Polymer* **1998**, *39*, 669−673. (c) Tinker, A. J.; George, M. H.; Barrie, J. A. Kinetics of the homopolymerization of vinylferrocene in dioxane in the presence of 2,2′-azobisisobutyronitrile. *J. Polym. Sci., Polym. Chem. Ed.* **1975**, *13*, 2133−2141.
(38) (a) Wrighton, M. S.; Thackeray, J. W.; Natan, M. J.; Smith, D. K.; Lane, G. A.; Bëlanger, D.; Albery, W. J.; Akhtar, M.; Lowe, C. R.; Higgins, I. J. Modification of microelectrode arrays: new microelectrochemical devices for sensor applications. *Philos. Trans. R. Soc., B* **1987**, *316*, 13−30. (b) Slattery, S. J.; Blaho, J. K.; Lehnes, J.; Goldsby, K. A. pH-Dependent metal-based redox couples as models for proton-coupled electron transfer reactions. *Coord. Chem. Rev.* **1998**, *174*, 391−416. (c) Costentin, C. Electrochemical Approach to the Mechanistic Study of Proton-Coupled Electron Transfer. *Chem. Rev.* **2008**, *108*, 2145−2179. (d) Gerken, J. B.; Pang, Y. Q.; Lauber, M. B.; Stahl, S. S. Structural Effects on the pH-Dependent Redox Properties of Organic Nitroxyls: Pourbaix Diagrams for TEMPO, ABNO, and Three TEMPO Analogs. *J. Org. Chem.* **2018**, *83*, 7323−7330.
(39) Blaho, J. K.; Goldsby, K. A. Redox regulation based on the pH-dependent hydrolysis of 2-pyridinecarboxaldehyde coordinated to ruthenium(II). *J. Am. Chem. Soc.* **1990**, *112*, 6132−6133.
(40) Katz, E.; de Lacey, A. L.; Fernandez, V. M. Covalent binding of viologen to electrode surfaces coated with poly(acrylic acid) prepared by electropolymerization of acrylate ions: II. Effect of the ionization

state of the polymeric coating on the formal potential of viologen. *J. Electroanal. Chem.* **1993**, *358*, 261−272.
(41) Tam, T. K.; Ornatska, M.; Pita, M.; Minko, S.; Katz, E. Polymer Brush-Modified Electrode with Switchable and Tunable Redox Activity for Bioelectronic Applications. *The Journal of Physical Chemistry C* **2008**, *112*, 8438−8445.
(42) Kang, H.; Liu, R.; Sun, H.; Zhen, J.; Li, Q.; Huang, Y. Osmium Bipyridine-Containing Redox Polymers Based on Cellulose and Their Reversible Redox Activity. *The Journal of Physical Chemistry B* **2012**, *116*, 55−62.
(43) Naegeli, R.; Redepenning, J.; Anson, F. C. Influence of supporting electrolyte concentration and composition on formal potentials and entropies of redox couples incorporated in Nafion coatings on electrodes. *J. Phys. Chem.* **1986**, *90*, 6227−6232.
(44) Tagliazucchi, M.; Williams, F. J.; Calvo, E. J. Effect of Acid−Base Equilibria on the Donnan Potential of Layer-by-Layer Redox Polyelectrolyte Multilayers. *J. Phys. Chem. B* **2007**, *111*, 8105−8113.
(45) Tagliazucchi, M.; Calvo, E. J.; Szleifer, I. Redox and Acid−Base Coupling in Ultrathin Polyelectrolyte Films. *Langmuir* **2008**, *24*, 2869−2877.
(46) (a) Liu, A.; Anzai, J.-I. Ferrocene-Containing Polyelectrolyte Multilayer Films: Effects of Electrochemically Inactive Surface Layers on the Redox Properties. *Langmuir* **2003**, *19*, 4043−4046. (b) Merchant, S. A.; Glatzhofer, D. T.; Schmidtke, D. W. Effects of Electrolyte and pH on the Behavior of Cross-Linked Films of Ferrocene-Modified Poly(ethylenimine). *Langmuir* **2007**, *23*, 11295−11302. (c) Molinero, V.; Calvo, E. J. Electrostatic interactions at self assembled molecular films of charged thiols on gold. *J. Electroanal. Chem.* **1998**, *445*, 17−25.
(47) Zhang, J.; Zhao, Y.; Yuan, C.-G.; Ji, L.-N.; Yu, X.-D.; Wang, F.-B.; Wang, K.; Xia, X.-H. Donnan Potential Caused by Polyelectrolyte Monolayers. *Langmuir* **2014**, *30*, 10127−10132.
(48) Hatozaki, O.; Anson, F. C. Diffusion Coefficients of Intrinsically Electroactive Polyelectrolytes and of Counterions Bound to Them. *J. Phys. Chem.* **1996**, *100*, 8448−8453.
(49) Kobayashi, N.; Anson, F. C. Effects of adsorption and association with multiply charged counterions on the electrochemical responses of an electroactive polyelectrolyte. *J. Electroanal. Chem.* **1997**, *421*, 99−104.
(50) Beulen, M. W. J.; van Veggel, F. C. J. M.; Reinhoudt, D. N. Coupling of acid−base and redox functions in mixed sulfide monolayers on gold. *Chem. Commun.* **1999**, *6*, 503−504.
(51) Koide, S.; Yokoyama, K. Electrochemical characterization of an enzyme electrode based on a ferrocene-containing redox polymer. *J. Electroanal. Chem.* **1999**, *468*, 193−201.
(52) Cheng, R.; Meng, F.; Deng, C.; Klok, H.-A.; Zhong, Z. Dual and multi-stimuli responsive polymeric nanoparticles for programmed site-specific drug delivery. *Biomaterials* **2013**, *34*, 3647−3657.
(53) Mao, X.; Simeon, F.; Achilleos, D. S.; Rutledge, G. C.; Hatton, T. A. Metallocene/carbon hybrids prepared by a solution process for supercapacitor applications. *J. Mater. Chem. A* **2013**, *1*, 13120−13127.
(54) (a) Dai, C.-A.; Liu, C.-P.; Lee, Y.-H.; Chang, C.-J.; Chao, C.-Y.; Cheng, Y.-Y. Fabrication of novel proton exchange membranes for DMFC via UV curing. *J. Power Sources* **2008**, *177*, 262−272. (b) Hogen-Esch, T. E.; Li, M.; Prakash, S. G. K. Method for the fabrication of homogenous blends of polystyrenesulfonic acid and polyvinylidene fluoride suitable for the application in direct oxidation methanol fuel cells (DMFCs). United States US10,586,995B2, 2020. (c) Mukhin, S. Blends of polystyrene sulfonic acid copolymers and polyvinylidene fluoride as polyelectrolyte membranes; PhD Thesis, University of Southern California: Los Angeles, 2016.
(55) (a) Lattuada, M.; Hatton, T. A. Functionalization of Monodisperse Magnetic Nanoparticles. *Langmuir* **2007**, *23*, 2158−2168. (b) Mori, H.; Müller, A. H. E. New polymeric architectures with (meth)acrylic acid segments. *Prog. Polym. Sci.* **2003**, *28*, 1403−1439.
(56) Crozier, A.; Moritz, T. Chapter 2 - Physico-chemical methods of plant hormone analysis. In *New Comprehensive Biochemistry*, Hooykaas, P. J. J., Hall, M. A., Libbenga, K. R. Eds.; Vol. 33; Elsevier, 1999; pp. 23−60.
(57) Deng, H.; Shen, W.; Gao, Z. Synthesis of water-soluble and cross-linkable ferrocenyl redox polymers for uses as mediators in biosensors. *Sens. Actuators, B* **2012**, *168*, 238−242.
(58) Mao, X.; Rutledge, G. C.; Hatton, T. A. Polyvinylferrocene for Noncovalent Dispersion and Redox-Controlled Precipitation of Carbon Nanotubes in Nonaqueous Media. *Langmuir* **2013**, *29*, 9626−9634.
(59) (a) Huang, X.-J.; Im, H.-S.; Lee, D.-H.; Kim, H.-S.; Choi, Y.-K. Ferrocene Functionalized Single-Walled Carbon Nanotube Bundles. Hybrid Interdigitated Construction Film for l-Glutamate Detection. *J. Phys. Chem. C* **2007**, *111*, 1200−1206. (b) Huang, R.-H.; Sun, C.-H.; Tseng, T.-M.; Chao, W.-K.; Hsueh, K.-L.; Shieu, F.-S. Investigation of Active Electrodes Modified with Platinum/Multiwalled Carbon Nanotube for Vanadium Redox Flow Battery. *J. Electrochem. Soc.* **2012**, *159*, A1579−A1586. (c) Gayathri, P.; Senthil Kumar, A. Electrochemical Behavior of the 1,10-Phenanthroline Ligand on a Multiwalled Carbon Nanotube Surface and Its Relevant Electrochemistry for Selective Recognition of Copper Ion and Hydrogen Peroxide Sensing. *Langmuir* **2014**, *30*, 10513−10521. (d) Hu, J.; Ji, Y.; Chen, W.; Streb, C.; Song, Y.-F. "Wiring" redox-active polyoxometalates to carbon nanotubes using a sonication-driven periodic functionalization strategy. *Energy Environ. Sci.* **2016**, *9*, 1095−1101.
(60) Tagliazucchi, M.; Grumelli, D.; Calvo, E. J. Nanostructured modified electrodes: Role of ions and solvent flux in redox active polyelectrolyte multilayer films. *Phys. Chem. Chem. Phys.* **2006**, *8*, 5086−5095.
(61) Calvo, E. J.; Wolosiuk, A. Donnan Permselectivity in Layer-by-Layer Self-Assembled Redox Polyelectrolye Thin Films. *J. Am. Chem. Soc.* **2002**, *124*, 8490−8497.
(62) Petrucci, R. H.; Harwood, W. S.; Madura, J. D. *General Chemistry: Principles and Modern Applications*; Pearson/Prentice Hall, 2007.
(63) Dong, H.; Du, H.; Qian, X. Prediction of pKa Values for Oligomethacrylic Acids Using Combined Classical and Quantum Approaches. *J. Phys. Chem. B* **2009**, *113*, 12857−12859.
(64) Rossini, E.; Bochevarov, A. D.; Knapp, E. W. Empirical Conversion of pKa Values between Different Solvents and Interpretation of the Parameters: Application to Water, Acetonitrile, Dimethyl Sulfoxide, and Methanol. *ACS Omega* **2018**, *3*, 1653−1662.
(65) De Santis, G.; Fabbrizzi, L.; Licchelli, M.; Pallavicini, P. Controlling the acidity of the carboxylic group by a ferrocene based redox switch. *Inorg. Chim. Acta* **1994**, *225*, 239−244.
(66) Matsue, T.; Evans, D. H.; Osa, T.; Kobayashi, N. Electron-transfer reactions associated with host-guest complexation. Oxidation of ferrocenecarboxylic acid in the presence of .beta.-cyclodextrin. *J. Am. Chem. Soc.* **1985**, *107*, 3411−3417.
(67) Quan, M.; Sanchez, D.; Wasylkiw, M. F.; Smith, D. K. Voltammetry of Quinones in Unbuffered Aqueous Solution: Reassessing the Roles of Proton Transfer and Hydrogen Bonding in the Aqueous Electrochemistry of Quinones. *J. Am. Chem. Soc.* **2007**, *129*, 12847−12856.
(68) Bard, A. J.; Faulkner, L. R. *Electrochemical Methods: Fundamentals and Applications, 2nd Edition*; John Wiley & Sons, Incorporated, 2000.
(69) Smith, C. P.; White, H. S. Voltammetry of molecular films containing acid/base groups. *Langmuir* **1993**, *9*, 1−3.
(70) Doblhofer, K.; Vorotyntsev, M. The Membrane Properties of Electroactive Polymer Films. In *Electroactive Polymer Electrochemistry: Part 1: Fundamentals*, Lyons, M. E. G. Ed.; Springer US, 1994; pp. 375−442.
(71) (a) Zhou, X.; Wei, C.; Li, M.; Qiu, S.; Li, X. Thermodynamics of vanadium−sulfur−water systems at 298K. *Hydrometallurgy* **2011**, *106*, 104−112. (b) Gustafsson, J. P. Vanadium geochemistry in the biogeosphere −speciation, solid-solution interactions, and ecotoxicity. *Appl. Geochem.* **2019**, *102*, 1−25.

(72) Regan, J.; Dushaj, N.; Stinchfield, G. Reducing Hexavalent Chromium to Trivalent Chromium with Zero Chemical Footprint: Borohydride Exchange Resin and a Polymer-Supported Base. *ACS Omega* **2019**, *4*, 11554−11557.